

**HIGH ENERGY PHYSICS**

**IDENTIFIED PARTICLE PRODUCTION IN NUCLEAR COLLISIONS  
AT RELATIVISTIC ENERGIES\***

OANA RISTEA<sup>1</sup>, ELENA GIUBEGA<sup>1</sup>, A. JIPA<sup>1</sup>, C. RISTEA<sup>1</sup>, C. BEȘLIU<sup>1</sup>, VALERICA BABAN<sup>1</sup>,  
A. BARZU<sup>1</sup>, A. SCURTU<sup>1</sup>, I. ABU-QUOAD<sup>1</sup>, S. PARAGINA<sup>1</sup>, FLORICA PARAGINA<sup>1</sup>

<sup>1</sup>University of Bucharest, Faculty of Physics, Bucharest, Romania  
E-mail: giubega\_elena@yahoo.com

*Received July 26, 2012*

*Abstract.* We present measurements of identified charged hadron production at different collision centralities from Au+Au collisions at RHIC energies. The mass and centrality dependence of apparent temperatures for the identified particles produced in the collision are shown and discussed. The results are also compared to previous measurements at various energies.

*Key words:* heavy ion collisions, quark-gluon plasma, effective temperature, collective flow.

## 1. INTRODUCTION

One of the major goals of high-energy heavy-ion research is to explore properties of strongly interacting matter, as it may undergo a phase transition into a system of deconfined quarks and gluons (quark-gluon plasma, QGP) [1–3]. There is a large amount of experimental data obtained in nuclear collisions in a wide range of energies that allow us to look for anomalies in energy dependence of particle production and the onset of deconfinement process [4]. Among the basic observables used are the transverse momentum spectra of produced particles as they provide valuable information on particle production mechanisms as well as dynamics of the produced matter. The spectral shape can be used to obtain the transverse radial flow as it is entirely generated during the collision and therefore reflects the collision dynamics and the system temperature at the thermal freeze-out [5].

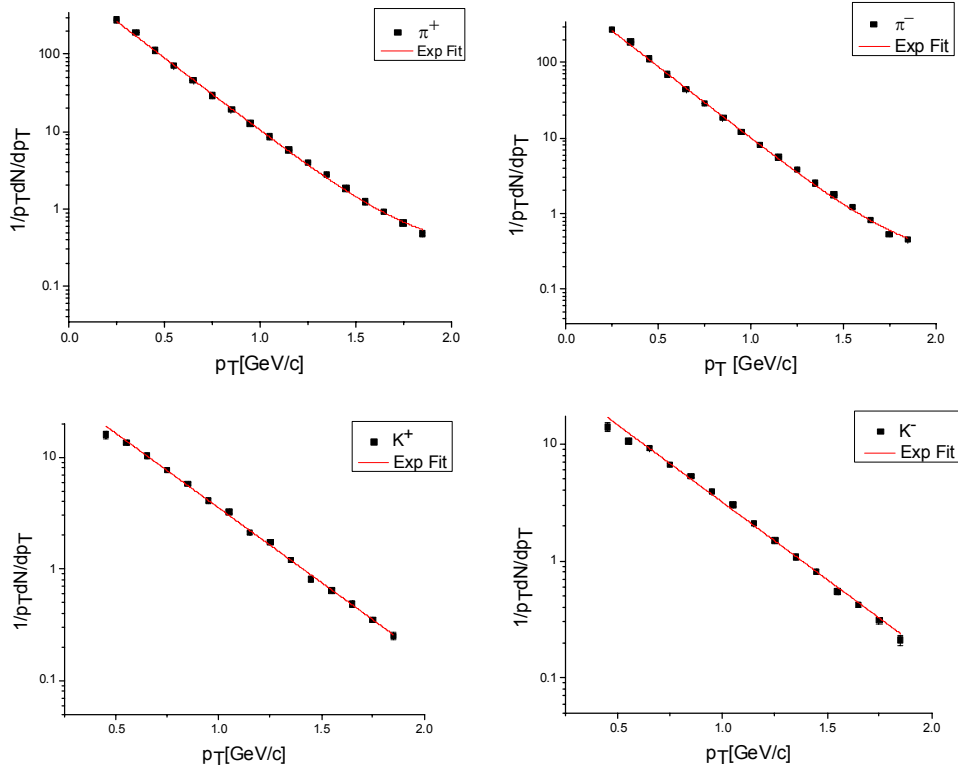
\* Paper presented at the Annual Scientific Session of Faculty of Physics, University of Bucharest, June 22–23, 2012, Bucharest-Magurele, Romania.

## 2. RESULTS AND DISCUSSION

The transverse momentum distributions for each particle species (charged pions, kaons, protons and antiprotons) measured by BRAHMS experiment in Au-Au collisions at  $\sqrt{s_{NN}} = 200$  GeV have been parameterized using the expression:

$$\frac{1}{2\pi p_T} \frac{d^2 N}{dp_T dy} = A \exp\left(-\frac{p_T}{T}\right), \quad (1)$$

where  $A$  is a normalization parameter that contains information on the rapidity density,  $T$  is the inverse slope parameter (it is called also the effective or apparent temperature) and  $p_T$  is the transverse momentum. BRAHMS [6] is one of the four experiments from the Relativistic Heavy Ion Collider (RHIC) [7]. The BRAHMS experiment consists of two movable spectrometers and a set of detectors used to determine global features of the collision such as the overall charged particle multiplicity, the collision vertex and the centrality of the collision.



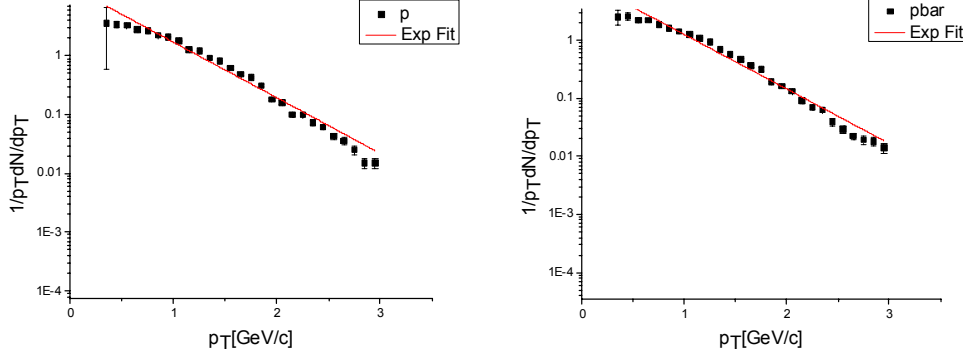


Fig. 1 – Transverse momentum spectra for  $\pi^+$ ,  $K^+$ ,  $p$  (left) and  $\pi^-$ ,  $K^-$ ,  $pbar$  (right) produced in central 0–10% Au-Au collisions at 200 GeV at midrapidity. Red lines represent the fit to the spectra with formula (1) in order to obtain the inverse slope parameters. Experimental data are taken from [8].

In Eq. (1),  $T$  and  $A$  are treated as free parameters and their values are extracted from fits to the spectra. The experimental data are shown in the Fig. 1. The apparent temperature is interpreted as due to the thermal motion coupled with a collective transverse flow of the fireball components assumed to be in thermal equilibrium. Collective motion, the flow, is the result of the collisions among the particles of the matter. The inverse slope parameters  $T$  from transverse momentum spectra are given in Table 1.

Table 1

The number of participants  $N_{part}$  and the apparent temperatures  $T$  for charged pions and kaons, protons and antiprotons in various centrality ranges

Parameter	Centrality 0–10%	Centrality 10–20%	Centrality 20–40%	Centrality 40–60%
$N_{part}$	328±6	239±10	140±11	62±10
$T(\pi^+)$ [MeV]	239±3	238±3	237±3	229±5
$T(\pi^-)$ [MeV]	235±3	234±4	233±4	227±1
$T(K^+)$ [MeV]	326±4	324±6	320±4	300±7
$T(K^-)$ [MeV]	329±7	321±4	319±6	300±9
$T(p)$ [MeV]	459±14	458±14	436±13	391±17
$T(p^{bar})$ [MeV]	463±13	457±14	443±12	377±12

The centrality dependence in the case of pions is weak and the apparent temperature is approximately constant. This result is consistent with the fact that the slope of the pion spectrum is not significantly changed by the collective expansion. The collective expansion is stronger in more central collisions. Since the pion apparent temperatures are lower, this fact suggests that the pion temperatures are the closest to the thermal freeze-out temperature.

The apparent temperatures for kaons, protons and antiprotons depend stronger on collision centrality. This dependency is stronger as the particles are heavier since the collective flow affects significantly higher mass particles.

The centrality dependence of the particle inverse slope parameters is shown in Fig. 2. Kaon values for central collisions are around  $\sim 325$  MeV and start to decrease as centrality increases and reach values around  $\sim 300$  MeV at 40–60% centrality. The decrease is  $\sim 10\%$  from central to (semi-)peripheral collisions and may be interpreted as due to the decrease of collective transverse flow as the centrality increases. The decrease of the inverse slopes for protons and antiprotons is around 20% from  $\sim 460$  MeV in most central collisions to  $\sim 380$ – $390$  MeV obtained in (semi-)peripheral collisions. Also, we observe the similarity between spectral features of  $K^+ - K^-$  and  $p - \bar{p}$ , respectively, and this may indicate that sources of particles and antiparticles have similar characteristics at all centralities covered by this analysis.

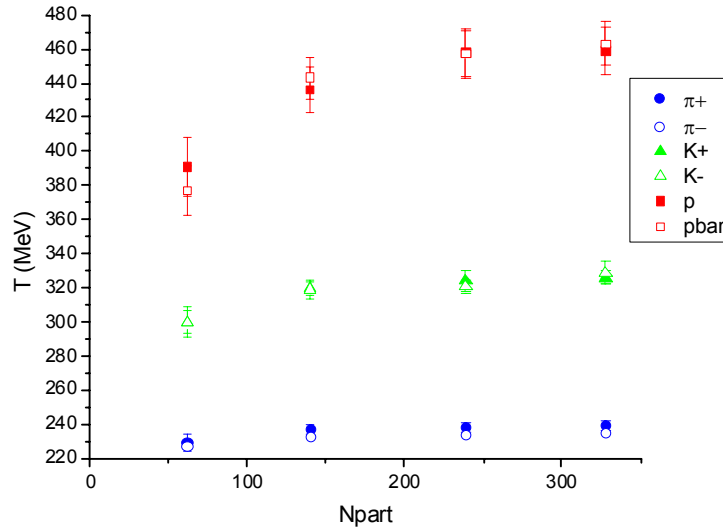


Fig. 2 – The apparent temperatures for  $\pi^+$ ,  $\pi^-$  (blue),  $K^+$ ,  $K^-$  (green points),  $p$  and antiprotons (red points) produced in Au-Au collisions at 200 GeV (this analysis) at midrapidity, as a function of the number of participants.

For Au-Au collisions at  $\sqrt{s_{NN}} = 62.4$  GeV, we obtain the apparent temperatures by fitting the transverse momentum spectra [9, 10] with the exponential expression above, for different types of particles detected by the BRAHMS experiment at midrapidity ( $y = 0$ ). The obtained values are listed in Table 2.

Table 2

The apparent temperatures for charged pions and kaons, protons and antiprotons as a function of collision energy

Parameter	$\sqrt{s_{NN}} = 200$ GeV	$\sqrt{s_{NN}} = 62.4$ GeV
$T(\pi^+)$ [MeV]	239±3	218±3
$T(\pi^-)$ [MeV]	235±3	214±3
$T(K^+)$ [MeV]	326±4	289±7
$T(K^-)$ [MeV]	329±7	300±6
$T(p)$ [MeV]	459±14	444±2
$T(p^{\text{bar}})$ [MeV]	463±13	430±2

The apparent temperatures obtained in Au-Au collisions at  $\sqrt{s_{NN}} = 62.4$  GeV are smaller than those obtained for Au-Au collisions at  $\sqrt{s_{NN}} = 200$  GeV. Pion apparent temperatures drop by  $\sim 20$  MeV, the kaon apparent temperatures decrease by  $\sim 30$  MeV and the temperatures for antiprotons decrease with  $\sim 35$  MeV. These results indicate that the nuclear matter produced in a 200 GeV Au-Au collision is "hotter" than the matter produced in a 62.4 GeV Au-Au collision. The difference is most visible for the heavier particles, strongly affected by the presence of collective transverse flow in the fireball.

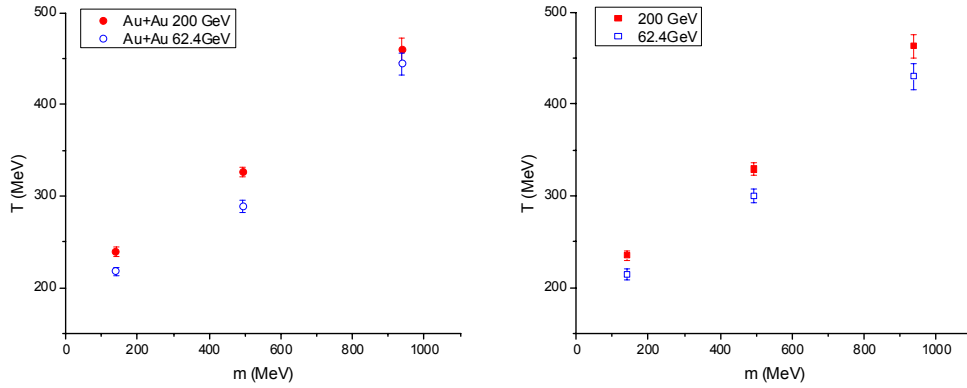


Fig. 3 – The apparent temperatures for  $\pi^+$ ,  $K^+$ ,  $p$  (left) and  $\pi^-$ ,  $K^-$ ,  $p^{\text{bar}}$  (right) obtained in most central 0–10% Au-Au collisions at 200 GeV and 62.4 GeV, as a function of the particle rest mass.

In Fig. 3 we observe that the apparent temperatures depend on the rest mass of particles, increasing with increasing mass and such behavior is a clear signal of collective flow in nuclear matter formed in collision.

Table 3

The energy dependence of the effective temperatures for charged pions and kaons produced in various heavy ion collisions

System	$\sqrt{s_{NN}}$ [GeV]	$T(\pi^+)$ [MeV]	$T(\pi^-)$ [MeV]	$T(K^+)$ [MeV]	$T(K^-)$ [MeV]
Au-Au	2.35	149±8	-	138±4	-
Au-Au	2.96	-	-	158±3	149±11
Au-Au	3.6	-	-	208±6	166±14
Au-Au	4.1	-	-	258 ±11	173±13
Au-Au	4.53	-	-	204 ±6	200±5
C-C	17	171±10	171±10	188±10	185±10
Si-Si	17	173±10	178±10	192±10	196±10
Pb-Pb	17	-	180±13	232±8	226±15
Au-Au	62.4	218±3	214±3	289 ±7	300±6
Au-Au	200	239±3	235±3	326 ±4	329±7
p-p	17.2	-	-	172 ± 17	164 ± 16
p-p	23	-	-	161.5 ± 4.9	150.7 ± 5.1
p-p	31	-	-	169.5 ± 5.2	145.8 ± 5.8
p-p	45	-	-	155 ± 4.9	161.8 ± 6.2
p-p	53	-	-	167.5 ± 5.2	177.8 ± 5.6
p-p	63	-	-	179.4 ± 13.8	185.6 ± 13.9

To study system and energy dependence of the apparent temperatures, we compare the results obtained in this analysis to those obtained in various nuclear collisions at different energies. In the Fig. 4 (left) the results on the apparent temperature of pions obtained in different heavy ion collisions are plotted as a function of  $\sqrt{s_{NN}}$ . In the right part of Fig. 4 are plotted the results on the apparent temperature of kaons obtained for p+p interactions [13–15] as a function of  $\sqrt{s_{NN}}$  together with the corresponding data for central Pb+Pb (Au+Au) collisions at AGS [16], SPS [17, 18] and RHIC.

At the same collision energy the apparent temperature is higher for larger system produced in the collision. For C + C and Si + Si collisions, the system size is small compared to Pb + Pb collision at the same energy, therefore the density of produced particles is smaller [12] and as a consequence the apparent temperatures are lower. For the same system, for example Au + Au, at different energies, the apparent temperatures are higher for higher energy. We obtain in this analysis the same behavior which shows that our results are consistent with other results.

It may be seen from Fig. 4 (right) that the apparent kaon temperatures obtained in proton-proton collisions do not depend on energy, while the temperatures obtained in heavy ion collisions increase with increasing energy. This confirms that in heavy ion collisions the produced matter develops collective flow that is even stronger when the energy is higher, while in p+p collisions the density of produced particles is smaller and hence the flow is weaker. Data from p+p collisions are taken from [13–15].

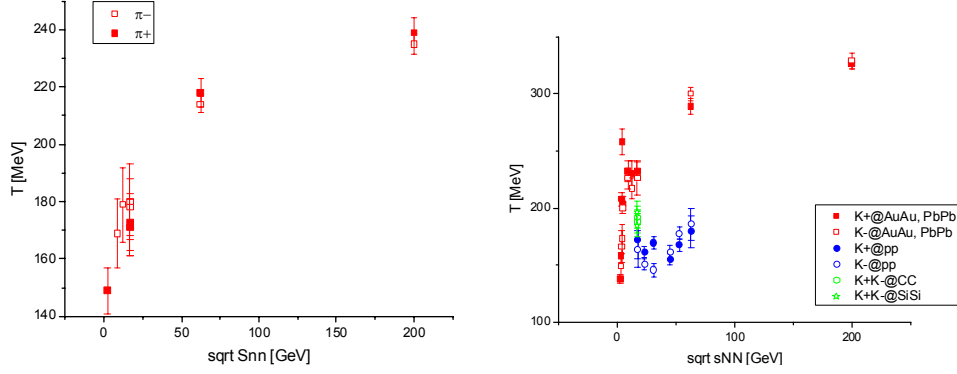


Fig. 4 – The apparent temperatures for  $\pi^+$ ,  $\pi^-$  (left) and  $K^+$ ,  $K^-$ , obtained in different types of collisions at various energies.

The dependence of the apparent temperature on the colliding energy is fitted with the expression:

$$T = a + b \cdot \ln(\sqrt{s_{NN}}), \quad (2)$$

where  $a$  and  $b$  are constant fit parameters and  $\sqrt{s_{NN}}$  is given in units of GeV [19]. The best fit to the data is presented in Fig. 5 and yields  $a = (124.2 \pm 11.3)$  MeV and  $b = (39.1 \pm 4.3)$  MeV. For Pb+Pb collisions at LHC energy of  $\sqrt{s_{NN}} = 2.76$  GeV our estimate for the kaon apparent temperature is around 434 MeV.

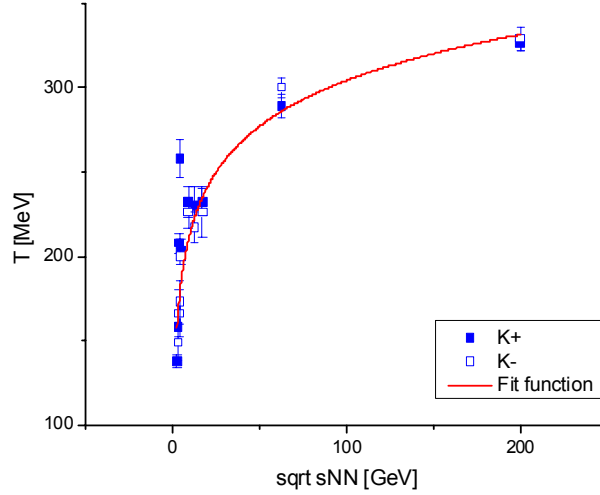


Fig. 5 – The apparent temperatures for  $K^+$  and  $K^-$  obtained in different heavy ion collisions at various energies. The logarithmic parameterization is indicated by solid line.

Measured kaon apparent temperature appears to form a plateau at lower energies before rising to significantly higher values for 62.4 GeV and 200 GeV. Such behavior is seen for A+A collisions but not for p+p collisions. If the system forms a mixed phase region, the early stage pressure and temperature are predicted to become independent of the energy density and this effect creates a plateau in the energy dependence of the pressure and temperature [20, 21]. Currently measurements at RHIC in the Beam Energy Scan Program (BES) are being done, in order to see how far this possible plateau extends, as this may signal the transition to QGP system.

### 3. CONCLUSIONS

In summary, we have analyzed transverse momentum spectra of charged identified particles produced in Au-Au collisions at 200 and 62.4 GeV. The inverse slope parameters for charged particles show a decrease with increasing centrality and may be interpreted as a consequence of the smaller transverse collective flow from a less dense local system. The apparent temperatures for pions and kaons obtained in heavy ion collisions increase with collision energy.

*Acknowledgements.* The work of Oana Ristea and Catalin Ristea was supported by the strategic grant POSDRU/89/1.5/S/58852, Project „Postdoctoral programme for training scientific researchers”, co-financed by the European Social Found within the Sectorial Operational Program Human Resources Development 2007-2013. The work of Valerica Baban was supported by the Project POSDRU/6/1.5/S/10, “Projected development and performance in doctoral research of interdisciplinary type“. This work was partially supported by PN-II-ID-PCE-IDEI 34/05.10.2011 grant.

### REFERENCES

1. Al. Jipa, C. Besliu, *Elemente de Fizică Nucleară Relativistă. Note de curs*, Editura Universității București, 2002.
2. E. Shuryak, Nucl.Phys.Proc.Suppl. **195**, 111 (2009);  
J.P. Blaizot, <http://arxiv.org/abs/hep-ph/01071311>;  
J. Rafelski, J. Letessier, Eur.Phys.J., **A29**, 107 (2006).
3. S. Sarkar, H. Satz, B. Sinha, *The physics of the Quark-Gluon Plasma. Lecture Notes in Physics*, Springer Verlag, 2010.
4. I. Arsene *et al.* [BRAHMS Collaboration], Nucl. Phys., **A757**, 1 (2005);  
B.B. Back *et al.* [PHOBOS Collaboration], Nucl. Phys., **A757**, 28 (2005);  
J. Adams *et al.* [STAR Collaboration], Nucl. Phys., **A757**, 102, (2005);  
K. Adcox *et al.* [PHENIX Collaboration], Nucl. Phys., **A757**, 184, (2005).
5. S. Reinhard *et al.*, *Relativistic Heavy Ion Collisions*, Springer Verlag, 2010.
6. M. Adamczyk *et al.* [BRAHMS Collaboration], Nucl. Inst. Meth., **A499**, 2–3, 437 (2003);  
R. Debbe *et al.*, Nucl. Inst. Meth., **A570**, 216, (2007);  
Y. K. Lee, R. Debbe, J. H. Lee, H. Ito and S. J. Sanders, Nucl. Instrum. Meth., **A516**, 281 (2004).

7. \*\*\* [www.bnl.gov/RHIC/](http://www.bnl.gov/RHIC/)
8. I. Arsene *et al.* [BRAHMS Collaboration], Phys. Rev., **C72**, 014908, (2005).
9. I. Arsene *et al.* [BRAHMS Collaboration], Phys. Lett., **B687**, 36-41 (2010).
10. I. Arsene *et al.* [BRAHMS Collaboration], Phys. Lett., **B677**, 267-271, (2009).
11. O. Ristea, Al. Jipa, C. Ristea, C. Besliu, S. Velica, Rom. Rep. Phys., **64**, 3 (2012).
12. S. Velica *et al.*, Rom. Rep. Phys., **64**, 3 (2012).
13. I. Kraus [NA49 Collaboration], arXiv: nucl-ex/0306022.
14. B. Alper *et al.* [British-Scandinavian Collaboration], Nucl. Phys., **B 100**, 237 (1975).
15. E. E. Zabrodin *et al.*, Phys. Rev., **D 52**, 1316 (1995).
16. L. Ahle *et al.* [E866 and E917 Collaborations], arXiv: nucl-ex/0008010; C. Ogilvie *et al.* [E866 Collaboration], arXiv: nucl-ex/9802004;  
L. Ahle *et al.* [E866 and E917 Collaborations], arXiv: nucl-ex/9910008.
17. \*\*\* NA49 Collaboration, Phys. Rev. Lett., **94**, 052301 (2005).
18. \*\*\*NA49 Collaboration, arXiv: nucl-ex/040603; NA49 Collaboration, arXiv: nucl-ex/0806.1937;  
NA49 Collaboration, arXiv: nucl-ex/0205002
19. M. Kliemant, B. Lungwitz, M. Gazdzicki, arXiv:hep-ex/0308002
20. M.M. Aggarwal *et al.* [STAR Collaboration], arXiv: nucl-ex/1007.2613.
21. M. Gazdzicki and M. I. Gorenstein, Acta Phys. Polon., **B30**, 2705 (1999), hep-ph/9803462.